Novel ternary AgCl/Bi_2WO_6/TiO_2 composites for enhanced photocatalytic activity

Y. H. Ding [a], Y. T. Zhang [a], J. L. Guo [a], Y. J. Duan [a], K. Lei [a], S. J. Hu [a], H. R. Dong [a], R. Xiong [b], Y. Sun [a, b, *]
[a] *School of Mechanical Engineering, Chengdu University, Chengdu 610106, China*
[b] *Sichuan Province Engineering Technology Research Center of Powder Metallurgy, Chengdu, 610106, China*

TiO_2 microspheres and Bi_2WO_6 microflowers were fabricated by hydrothermal method and then in-situ deposited with AgCl particles to form a ternary AgCl/Bi_2WO_6/TiO_2 (ABT) heterojunction. Compared with pure AgCl, Bi_2WO_6, and TiO_2, with the mass ratio 4:1:4, ternary heterojunction exhibited the highest photocatalytic performance, achieving 99.4% removal efficiency of Rhodamine B (RhB) in 30 min. The improved degradation efficiency was ascribed to the formation of heterojunctions, which reduced the combination of photogenerated carriers and accelerated their separation and transfer.

(Received September 16, 2024; Accepted November 25, 2024)

Keywords: Bi_2WO_6 microflowers, AgCl; TiO_2 microspheres, Photocatalysis

1. Introduction

At present, the textile industry is developing rapidly, dyeing wastewater could cause harm to the environment and human health. Photocatalytic degradation technology can decompose dyes by sunlight, and has broad application prospect in dyeing wastewater treatment [1,2]. Bismuth tungstate (Bi_2WO_6), a n-type catalyst with appropriate bandgap structure, has received extensive attention [3]. However, the existent insufficiency of Bi_2WO_6 such as poor visible light absorption, small surface area, and fast recombination of carriers [4] restricted its application. For enhancing its photocatalytic activity, a large number of methods have been used to decorate Bi_2WO_6, including doping and coupling [5]. TiO_2 is a popular photocatalyst owing to its stabilization, non-toxicity and low cost [6]. Therefore, the combination of TiO_2 and Bi_2WO_6 to synthesize heterojunction is an effective way to degrade organic pollutants [7].

So far, Ag/AgCl photocatalyst is used to degrade wastewater [8] and loading Ag/AgCl on other catalysts is a simple method to achieve higher degradation of organic wastewater, such as Ag/AgCl/TiO_2 [9] and Ag/AgCl/$BiOIO_3$ [10]. In our previous research work, Bi_2WO_6/TiO_2 and AgCl/Bi_2WO_6 heterojunction have been prepared and demonstrated superior photocatalytic performance[11,12]. Hence, it is expected that decorating Bi_2WO_6/TiO_2 composites with AgCl might boost the photocatalytic degradation efficiency.

In this work, AgCl/Bi_2WO_6/TiO_2 ternary heterojunction was designed and synthesized by hydrothermal and in-situ deposition method. Compared with pure AgCl, Bi_2WO_6 and TiO_2, AgCl/Bi_2WO_6/TiO_2 composites showed higher photocatalytic performance. The results revealed that the separation and transfer of carriers was accelerated by ternary heterojunction structure.

2. Experimental

2.1. Synthesis of AgCl/Bi_2WO_6/TiO_2 composites

Bi_2WO_6 microflowers were synthesized via hydrothermal method. 0.66 g of $Na_2WO_4 \cdot 2H_2O$ and 1.94 g of $Bi(NO_3)_3 \cdot 5H_2O$ were added in 30 and 40 mL deionized water, named A and B, respectively. Subsequently, solution A and solution B were mixed, and moved to a Teflon-lined autoclave (100 mL), heating at 180°C for 24 h.

* Corresponding author: sunyan@cdu.edu.cn
https://doi.org/10.15251/DJNB.2024.194.1807

Self-assembly TiO_2 microspheres were prepared by hydrothermal method. 10 mL of butyl titanate was slowly dripped into the mixture solution, including 10 mL HCl and 10 mL deionized water. Subsequently, the solution was put in a Teflon-lined autoclave (50 mL), heating at 180℃ for 12 h.

$AgCl/Bi_2WO_6/TiO_2$ composite were prepared by in-situ deposition method. Bi_2WO_6 and TiO_2 powders with mass ratio of 1:4 were mixed in 40 mL ethanol with stirring. After drying, Bi_2WO_6/TiO_2 was dispersed in 0.05 mol/L $AgNO_3$ solution with stirring, followed by the addition of 0.05 mol/L KCl solution. After drying, the precipitate with a mass ratio of AgCl: Bi_2WO_6:TiO_2=4:1:4 was obtained and denoted as ABT.

2.2. Characterization

DX-2700B X-ray diffractometer (XRD) was utilized to characterize crystal structure. The microstructure of products was observed via a Sigma 300 scanning electron microscope (SEM). Valence band (VB) and elemental states of the catalysts were accomplished by a Thermo Scientific K-Alpha spectrometer with AlKα radiation. UV-vis DRS were recorded utilizing a TU-190 spectrophotometer. Photoluminescence (PL) spectra were analyzed by a FLS1000 spectrophotometer. BET measurements were carried out on a V-Sorb 2800P analyzer. Electron spin resonance (ESR) analysis to detect superoxide anion and hydroxyl radicals was performed using a Bruker ELEXSYS II E 500 apparatus.

2.3. Photocatalytic test

Photocatalytic degradation of RhB under 500 W Xe lamp irradiation. 100 mg of catalyst was placed in 100 mL RhB solution (10 mg/L) and stirred for 0.5 h without light. During the photocatalytic reaction, the suspension was sampled every 5 minutes and remove the powder and detected by a UV-vis spectrometer. Besides, 1 mM of ethylenediamine tetraacetic acid (EDTA), 1 mM of benzoquinone (BQ) and 10 mM of tertiary butanol (TBA) were added as radical scavengers in the capture experiments.

3. Results and discussion

Fig. 1 displays XRD patterns of Bi_2WO_6, TiO_2, AgCl, and ABT catalysts. The peaks of TiO_2 located at 2θ =27.5°, 36.1°, 41.2°, 54.3°and 56.6° belong to (110), (101), (111), (211) and (220) crystal planes and match well with rutile phase TiO_2. All peaks of prepared Bi_2WO_6 sample completely accord with the quadrature-phase of Bi_2WO_6 [13]. The peaks at 2θ = 27.8°, 32.2°, 46.2°, 54.8°, 57.4° and 67.4° are indexed to (111), (200), (220), (311), (222) and (400) planes of AgCl [14]. Obviously, all peaks of AgCl, Bi_2WO_6 and TiO_2 are found in the XRD pattern of ABT, meaning the ternary composites were successfully synthesized. Additionally, the weak peaks of Bi_2WO_6 are attributed to the low proportion of Bi_2WO_6 in the composites.

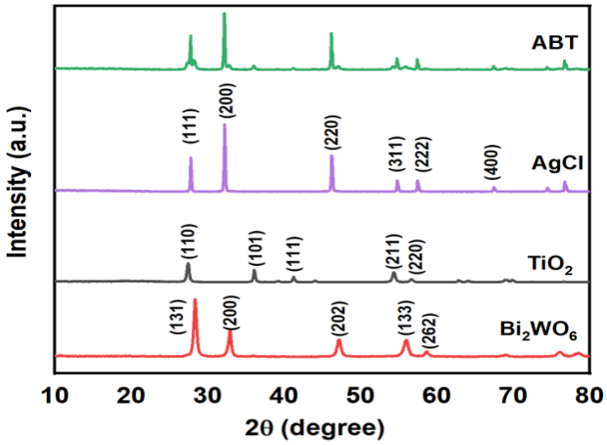

Fig. 1 XRD patterns of Bi_2WO_6, TiO_2, AgCl, and ABT catalysts

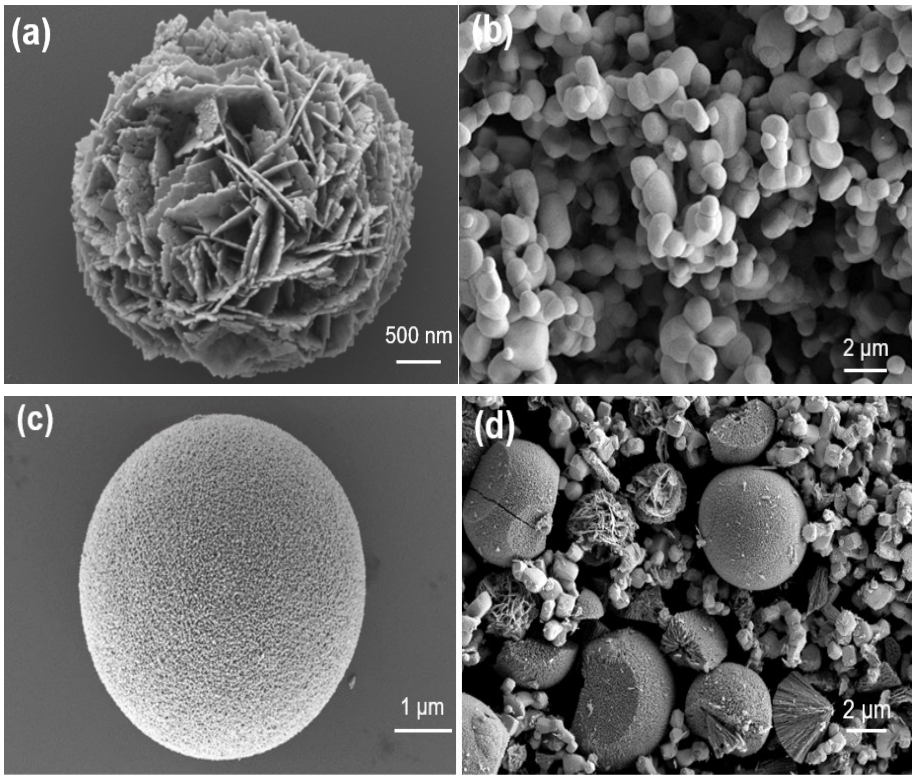

Fig. 2 SEM images: (a) Bi_2WO_6, (b) AgCl, (c) TiO_2 and (d) ABT.

The surface morphology of TiO_2, Bi_2WO_6, AgCl and ABT were analyzed by SEM. In Fig. 2a, Bi_2WO_6 demonstrates a flower-like microsphere structure with diameter of about 3-4 μm. It could be observed in Fig. 2b that pure AgCl is irregular particles with smooth surface. In Fig. 2c, TiO_2 exhibits a three-dimensional sphere structure composed of nanorods, and the diameter is about 5-6 μm. In the ternary composites (Fig. 2d), AgCl particles are attached to the surface of Bi_2WO_6 microflowers and TiO_2 microspheres, implying the successful preparation of ABT heterostructure. In addition, the specific surface areas of TiO_2, Bi_2WO_6, AgCl, and ABT are 27.6 m^2/g, 15.9 m^2/g and 4.6 m^2/g and 13.1 m^2/g, respectively.

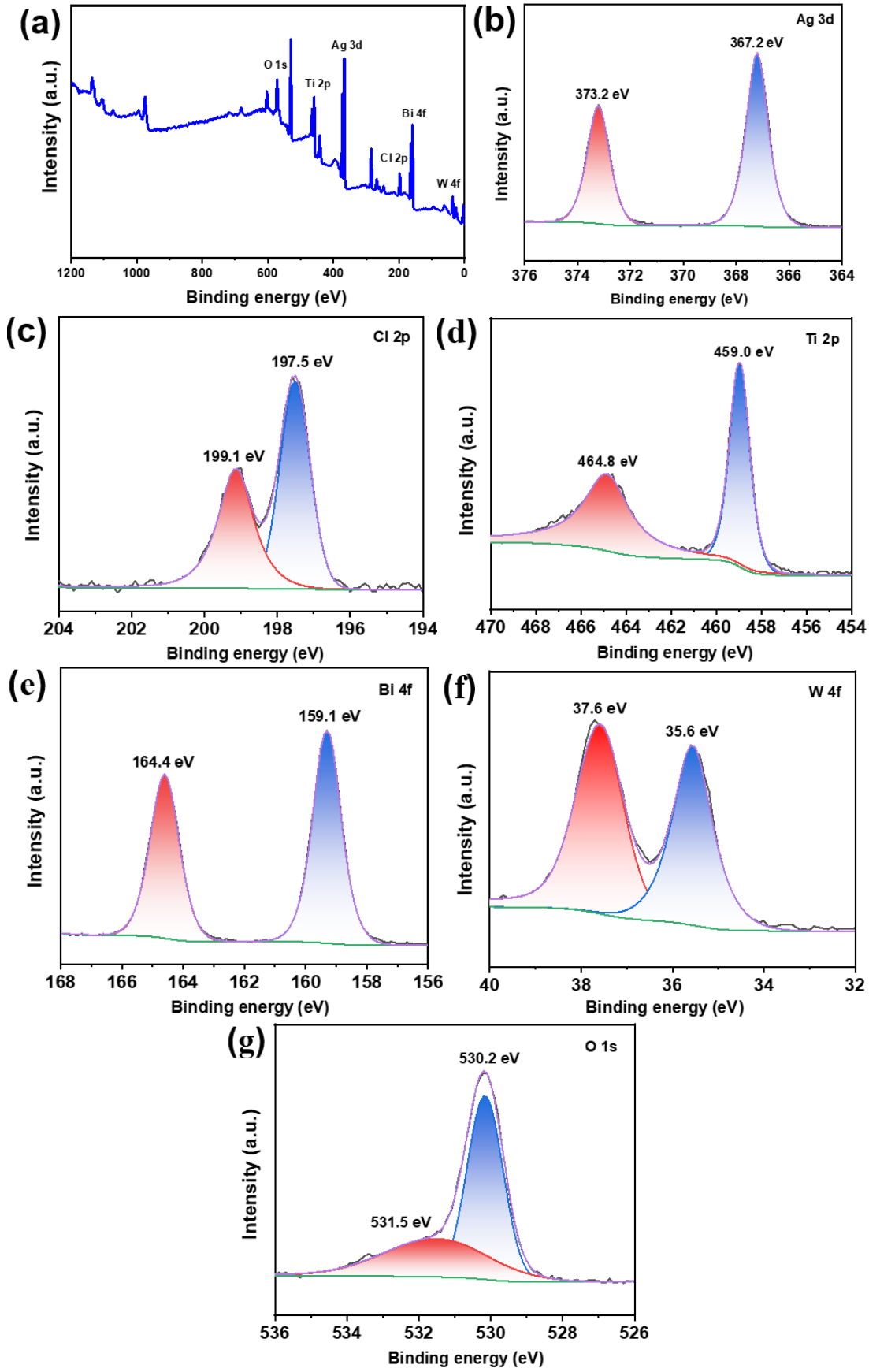

Fig. 3 XPS patterns of ABT sample: (a) full spectrum, (b) Ag 3d, (c) Cl 2p, (d) Ti 2p, (e) Bi 4f, (f) W 4f and (g) O 1s.

Fig. 3a displays the full spectrum of ABT catalyst. In Fig. 3b, the peaks at 367.2 and 373.2 eV in ABT belong to $Ag_{5/2}$ and $Ag_{3/2}$ of Ag^{+} [15]. In Fig. 3c, two peaks appeared at 199.1 and 197.5 eV correspond to Cl $2p_{1/2}$ and Cl $2p_{3/2}$ [16]. The peaks located at 459.0 and 464.8 eV (Fig.3d) could be indexed to Ti $2p_{3/2}$ and Ti $2p_{1/2}$ of Ti^{4+} [17]. As seen in Fig. 3e, the two peaks of Bi 4f located at 159.1 and 164.4 eV match well with Bi $4f_{7/2}$ and Bi $4f_{5/2}$ of Bi^{3+} [18]. The peaks of W 4f in Fig.3f at 37.6 and 35.6 eV are assigned to W $4f_{7/2}$ and W $4f_{5/2}$ [19], confirming the existence of W^{6+}. For O 1s (Fig. 3g), two peaks at 530.2 eV and 531.5 eV are attributed to Ti–O and W–O [20], respectively.

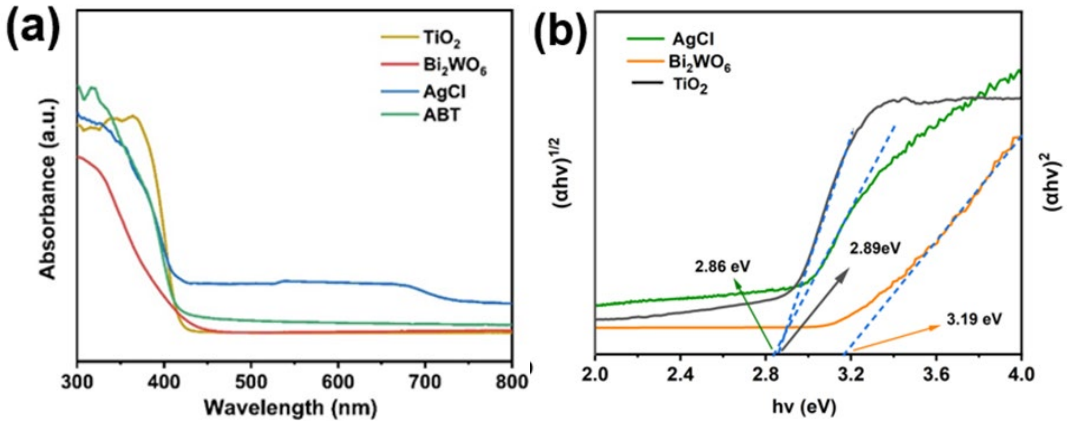

Fig. 4 (a) UV-vis DRS spectra of samples, (b) the bandgap of AgCl, Bi_2WO_6 and TiO_2.

Fig. 4a shows the optical properties of different catalysts. Compared with Bi_2WO_6 and TiO_2, the visible light absorption of ABT photocatalyst is enhanced after the deposition of AgCl. This enhanced light absorption could generate more electron-hole pairs in the degradation reaction. The bandgap could be achieved utilizing the formula $\alpha h\nu = A(h\nu - E_g)^{n/2}$ [22], and the Eg value of AgCl, Bi_2WO_6 and TiO_2 is 2.86, 3.19 and 2.89 eV (Fig. 4b), respectively.

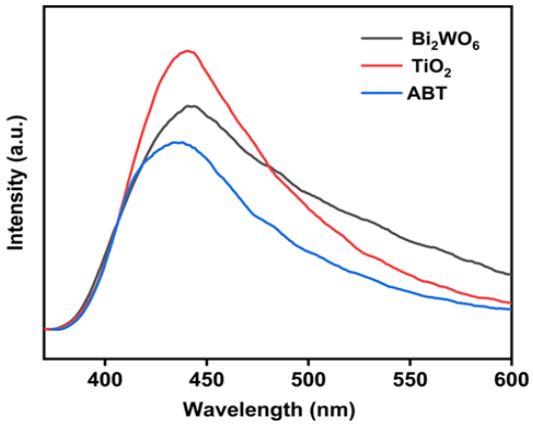

Fig. 5. PL spectra.

The PL spectra of pure Bi_2WO_6, TiO_2 and ABT composites are shown in Fig. 5. Generally, under the same experimental conditions, stronger PL peak intensity implies higher recombination rate of carriers. Compared with Bi_2WO_6 and TiO_2, the emission intensity of the ABT ternary heterojunction is the lowest, indicating that the heterojunction could reduce the combination of photogenerated carriers and accelerate their separation and transfer, finally enhancing the photocatalytic activity.

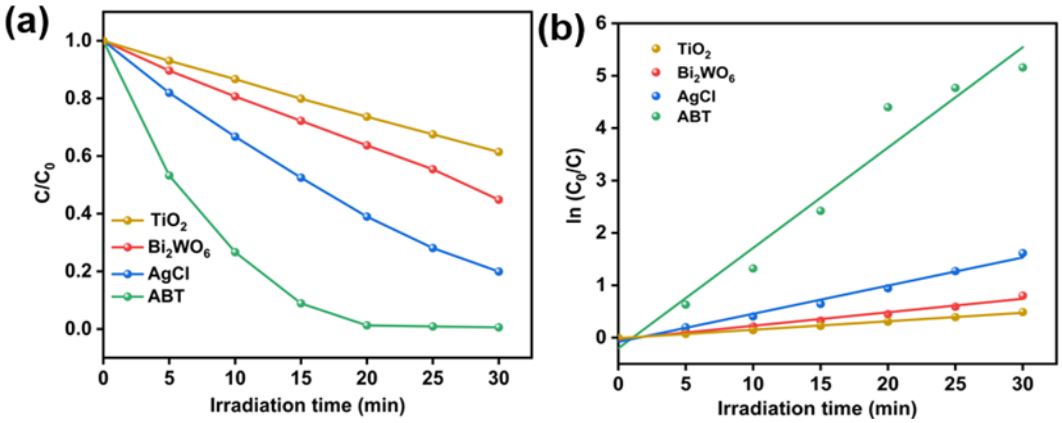

Fig. 6. (a) Photocatalytic degradation of RhB, (b) first-order kinetic curves.

Fig. 6a shows the photocatalytic properties of different samples. After 30 min, the degradation rate of RhB over pristine TiO_2, Bi_2WO_6, and AgCl is 38.6%, 55.2% and 80.1%, respectively. Owing to the construction of ternary heterojunction between AgCl, Bi_2WO_6 and TiO_2, the removal efficiency of RhB significantly increases to 99.4% within 30 min. The above results indicate that ternary heterojunction could accelerate the transfer of charge carriers, leading to the increase of degradation efficiency of RhB. The kinetic curves are given in Fig. 6b. The reaction constant of ABT is 0.1537 min^{-1}, which is higher than that of Bi_2WO_6 (0.0098 min^{-1}), TiO_2 (0.0065 min^{-1}) and AgCl (0.0301 min^{-1}).

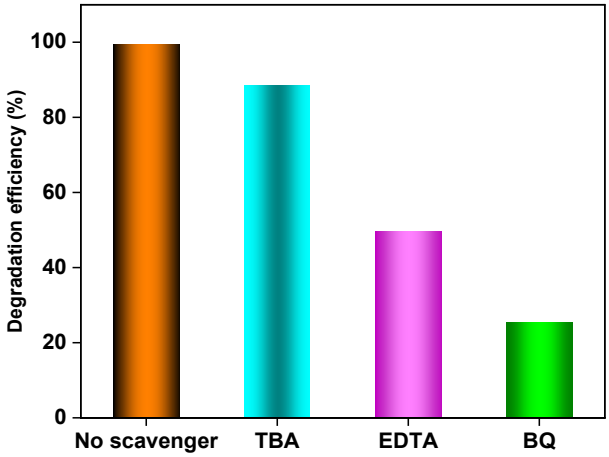

Fig. 7. Trapping experiments of ABT.

It could be found in Fig. 7 that after adding EDTA and BQ to degradation system, RhB removal efficiency declines significantly from 99.4 % to 25.4 % and 49.6 %, respectively. After the addition of TBA, only a little decrease can be observed and the removal efficiency is 88.5%. The results reveal that h^+ and $\cdot O_2^-$ play principal roles during the RhB degradation reaction.

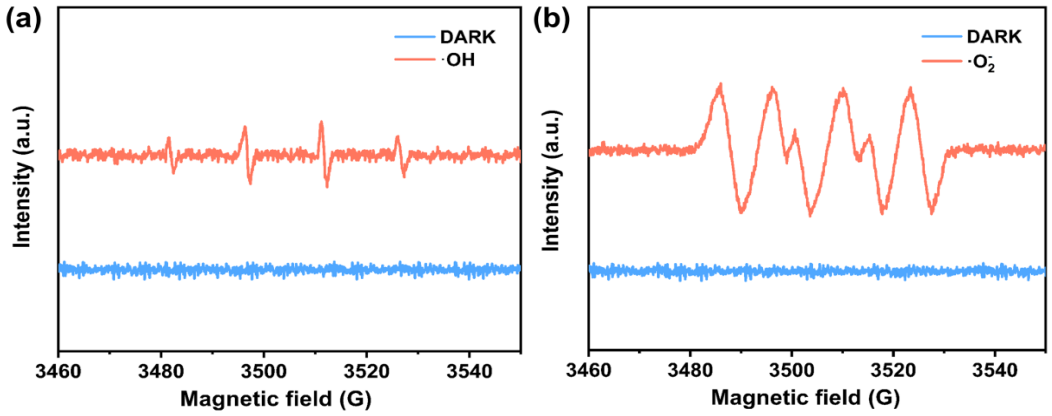

Fig. 8. ESR spectra of (a) ·OH and (b) ·O_2^-.

The results of ESR test are depicted in Fig. 8. As seen in Fig. 8a, no characteristic peak of ·OH can be found in the dark. After 5 min of illumination, the signals of ·OH could be seen clearly, indicating more ·OH were produced by ABT catalyst under illumination. Similarly, obvious characteristic peaks of $\cdot O_2^-$ are found in Fig. 8b after 5 min of illumination that is in accordance with the result of capture experiments.

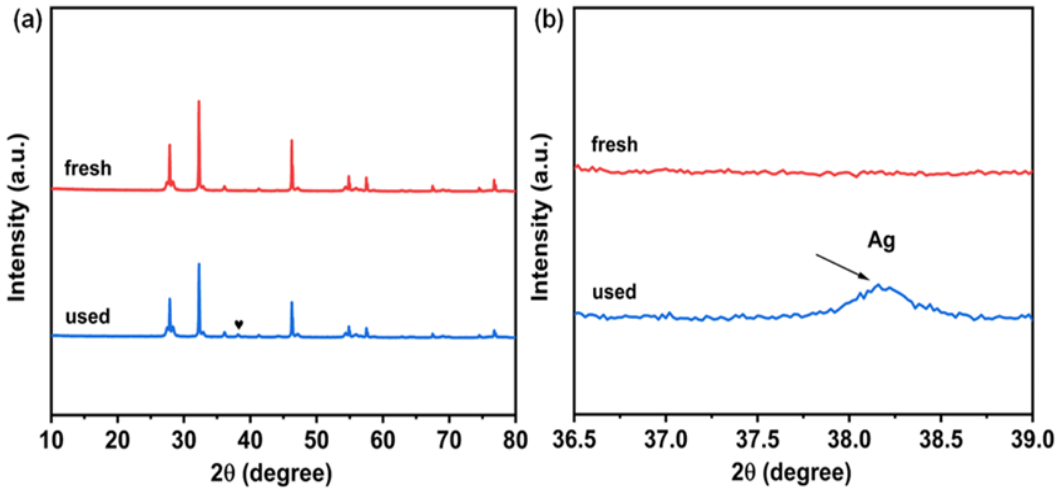

Fig. 9. XRD patterns of ABT before and after illumination.

To further explore the photocatalytic mechanism, XRD patterns of fresh and used $AgCl/Bi_2WO_6/TiO_2$ are displayed in Fig. 9. It is noticed that a new peak at $2\theta = 38.2°$ appears after illumination, which corresponds to Ag^0 nanoparticles reduced from AgCl during photocatalytic reaction.

The photocatalytic mechanism of RhB over $AgCl/Bi_2WO_6/TiO_2$ composites is inferred in Fig. 10. When ABT catalyst is irradiated by a simulated light source, electrons can be activated and transfer from valence band to conduction band (CB). During the photocatalytic reaction, a portion of AgCl could be reduced and generate Ag nanoparticles. As an electron bridge, Ag induces electrons to migrate from the AgCl to Bi_2WO_6. As CB potential of Bi_2WO_6 (-0.76 eV) is lower than $O_2/\cdot O_2^-$

potential (-0.33eV) [23], O_2 could be reduced to $\cdot O_2^-$, thereby degrading RhB. Meanwhile, e^- on CB of TiO_2 can move to VB of Bi_2WO_6 and couple with h^+. Moreover, valence band potential of TiO_2 (2.67eV) and AgCl (2.62 eV) are higher than $OH^-/\cdot OH$ potential (+2.40 eV), so a portion of holes gathered on VB of TiO_2 and AgCl can generate $\cdot OH$. Due to the strong oxidizing property, the holes remained on VB of TiO_2 and AgCl could immediately join the reaction and decompose RhB into small molecules. The formed ternary ABT composites could remarkably facilitate the separate and transfer of carriers, and boost the photocatalytic ability.

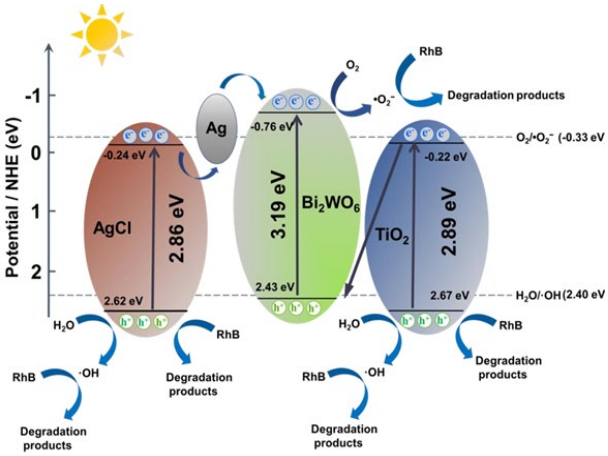

Fig. 10. Photocatalytic mechanism.

4. Conclusion

A simple and effective approach was designed to synthesize $AgCl/Bi_2WO_6/TiO_2$ ternary heterojunction. When the mass ratio was 4:1:4, ABT composites exhibited excellent degradation performance compared with pure TiO_2, AgCl and Bi_2WO_6. Characterization experimental results clarified the close contact of Bi_2WO_6, TiO_2 and AgCl could decline the combination of photogenerated carriers. Furthermore, the existence of $\cdot O_2^-$ and h^+ is proved in photocatalytic reaction and the charge transfer route of ABT composites was analyzed.

Acknowledgments

This research was supported by the Opening Project of Material Corrosion and Protection Key Laboratory of Sichuan province (No. 2023CL01).

References

[1] K. A. Adegoke, O. R. Adegoke, A. O. Araoye, J. Ogunmodede, O. S. Agboola, O. S. Bello, Bioresour. Technol. Rep. 18, 101082 (2022); https://doi.org/10.1016/j.biteb.2022.101082

[2] S. Muhammad, M. Majid, H. Attaul, A. Nadia, Environ. Sci. Pollut. Res. 29, 293-311 (2022); https://doi.org/10.1007/s11356-021-16389-7

[3] Y. Gao, S. Liu, Y. Wang, P. Zhao, K. Li, J. He, S. Liu, J. Colloid Interface Sci. 579, 177-185

(2020); https://doi.org/10.1016/j.jcis.2020.06.018

[4] C. L, X. Li, Q. Wu, J. Li, L. Wen, Y. Dai, B. Huang, B. Li, Z. Lou, ACS Nano. 15, 3529-3539 (2021); https://doi.org/10.1021/acsnano.1c00452

[5] Z. Jiao, Y. Tang, P. Zhao, S. Li, T. Sun, S. Cui, L. Cheng, Mater. Res. Bull. 113, 241-249 (2019); https://doi.org/10.1016/j.materresbull.2019.02.016

[6] Y. Zhou, F. Shen, S. Zhang, Q. Zhao, Z. Xu, H. Chen, ACS Appl. Mater. Interfaces. 12, 29876-29882 (2020); https://doi.org/10.1021/acsami.0c01064

[7] L. Zhang, G. Meng, B. Liu, X. Ge, J. Mol. Liq. 360, 119427 (2022); https://doi.org/10.1016/j.molliq.2022.119427

[8] S. Zhao, Y. Zhang, Y. Zhou, K. Qiu, C. Zhang, J. Fang, X. Sheng, J. Photochem. Photobiol. 350, 94-102 (2018); https://doi.org/10.1016/j.jphotochem.2017.09.070

[9] M. Maneshi, P. Cerruti, A. Moeini, M. Davoodi, Adv. Powder Technol. 33, 103808 (2022); https://doi.org/10.1016/j.apt.2022.103808

[10] T. Xiong, H. Zhang, Y. Zhang, F. Dong, Chin. J. Catal. 36, 2155-2163 (2015); https://doi.org/10.1016/S1872-2067(15)60980-9

[11] Y. Zhang, D. Wang, X. Luo, K. Lei, L. Mao, Y. Duan, X. Zeng, G. Wan, Q. Zhao, Y. Sun, Dig. J. Nanomater. Biostruct. 19, 571-579 (2024);

[12] Y. Zhang, D. Wang, X. Luo, Y. Chen, K. Lei, L. Mao, Y. Duan, X. Zeng, G. Wan, Q. Zhao, Y. Sun, Inorg. Chem. Commun. 165, 112543 (2024); https://doi.org/10.1016/j.inoche.2024.112543

[13] Y. Huang, S. Kang, Y. Yang, H. Qin, Z. Ni, S. Yang, X. Li, Appl. Catal. B. 196, 89-99 (2016); https://doi.org/10.1016/j.apcatb.2016.05.022

[14] X. Wen, C. Shen, C. Niu, D. Lai, M. Zhu, J. Sun, Y. Hu, Z. Fei, J. Mol. Liq. 288, 111063 (2019); https://doi.org/10.1016/j.molliq.2019.111063

[15] R. A. Senthil, S. Osman, J. Pan, M. Sun, A. Khan, V. Yang, Y. Sun, Colloids Surf. A. 567, 171-183 (2019); https://doi.org/10.1016/j.colsurfa.2019.01.056

[16] X. Li, S. Fang, L. Ge, C. Han, P. Qiu, W. Liu, Appl. Catal. B. 176-177, 62-69 (2015); https://doi.org/10.1016/j.apcatb.2015.03.042

[17] P. Karthik, P. Gowthaman, M. Venkatachalam, M. Saroja, Inorg. Chem. Commun. 119, 108060 (2020); https://doi.org/10.1016/j.inoche.2020.108060

[18] Y. Zhu, Y. Wang, Q. Ling, Y. Zhu, Appl. Catal. B. 200, 222-229 (2017); https://doi.org/10.1016/j.apcatb.2016.07.002

[19] S. Li, S. Hu, W. Jiang, Y. Liu, J. Liu, Z. Wang, J. Colloid. Interface. Sci. 501, 156-163 (2017); https://doi.org/10.1016/j.jcis.2017.04.057

[20] Q. Wang, Q. Lu, L. Yao, K. Sun, M. Wei, E. Guo, Dyes Pigm. 149, 612-619 (2018); https://doi.org/10.1016/j.dyepig.2017.11.028

[21] Q. Zhao, S. Liu, S. Chen, B. Ren, Y. Zhang, X. Luo, Y. Sun, Chem. Phys. Lett. 805, 139908 (2022); https://doi.org/10.1016/j.cplett.2022.139908

[22] L. Yuan, H. Deng, S. Li, S. Wei, J. Luo, Phys. Rev. B. 98, 24 (2018);

https://doi.org/10.1103/PhysRevB.98.245203

[23] M. Kohantorabi, G. Moussavi, P. Oulego, S. Giannakis, Appl. Surf. Sci. 555, 149692 (2021); https://doi.org/10.1016/j.apsusc.2021.149692